Journal of Thermal Analysis and Calorimetry, Vol. 82 (2005) 447–455

THE CALCULATION OF HEAT CAPACITY CURVES AND PHASE DIAGRAMS BASED ON REGULAR SOLUTION THEORY

P. Garidel[*]*, C. Johann and A. Blume*

Martin-Luther-University Halle/Wittenberg, Institute of Physical Chemistry, Mühlpforte 1, 06108 Halle/Saale, Germany

The intermolecular interactions of molecules within the bilayer are responsible for the lipid organisation, e.g. domain formation, and the interaction and stabilisation of proteins within the lipid matrix. The mixing behaviour of lipids, which reflects the intrinsic molecular interactions, can be deduced from the shape of the phase diagram (temperature *vs*. mole fraction diagram), which is constructed from the analysis of heat capacity curves obtained by DSC. However, there are no objective procedures to determine the temperatures corresponding to the border lines of the coexistence region, i.e. the liquidus and solidus curves of the phase diagram. The main challenge to overcome is to develop an objective method for the correct determination of the onset and offset temperatures of the melting curve for every single transition curve in a standardized manner.

The presented paper describes a procedure for the simulation of heat capacity curves. In a second step, based on the results from the heat capacity curve simulation, a phase diagram is calculated using a non-ideal, non-symmetric mixing model. The non-ideality parameters obtained from the calculation describe the intermolecular interaction of both components in a single phase region. Using this procedure, examples of the mixing behaviour of various binary phospholipid systems are analysed and it is shown how the mixing behaviour is influenced by external factors like e.g. the pH or ionic strength.

Keywords: *calorimetry, DSC, lipid organization, non-ideal mixing, non-ideality parameter, phase diagram, phospholipids*

Introduction

From their studies of erythrocytes, Gorter and Grendel (1925) concluded that the erythrocyte membrane contains sufficient lipid to provide a lipid bilayer matrix surrounding the 'red' cell [1]. The resulting concept that the major functional role of lipids is providing a bilayer permeability barrier between external and cellular (internal) compartments was long ago a major topic for membranologists. This concept has been developed and used for the encapsulation of active ingredients in liposomes, the latter serving as a drug delivery system [2]. An important observation was the fact that membranes are 'fluid' (fluid-mosaic model according to Singer and Nicholson [2, 3]), allowing rapid lateral diffusions in the plane of the membrane. Additionally, it was found that proteins are often inserted into and through the lipid bilayer membrane, and that the bioactivities of many proteins require a distinct micro-environment (i.e. phase state) in the membrane for optimal protein function, some requiring a fluid environment, whereas others require more rigid surroundings [3]. These observations were derived from studies of bacterial systems. Saturated as well as unsaturated fatty acids were identified to be essential for the regulation of various membrane properties. Additionally, it was observed that the lipids present in the membrane are found in the gel phase as well as in the liquid-crystalline phase. Thus, the phase behaviour of the membrane lipids determines the biological membrane function. Additionally, it was found that inhomogeneities [4, 5] like liquid–liquid immiscibilities [6, 7] or other micro-domain formation play a relevant role in various biological functions [3]. So-called 'lipid rafts', micro-domains of particular lipid composition, as an example, are conceived to be a part of a mechanism for the intracellular trafficking of lipids and lipid-anchored proteins [8–13].

Biological membranes are composed of an astonishing variety of amphiphilic molecules, like various phospholipids or fatty acids [3, 14, 15]. The huge lipid diversity as found in biological membranes suggests particular functional roles for each component. However, elucidation of these functional roles for individual lipid species is still a challenge.

An attempt for understanding the role of single lipid components in biological membranes is the use of model membranes composed of only a small number of lipids. Various biophysical properties of the model membrane are studied, by varying the amount of one component of the system. The presence of different lipids determines the physical behaviour of the lipid barrier and thus the phase state. The simplest systems are binary phospholipid mixtures. However, even in such 'simple' systems small variations of the buffer pH or the presence of e.g. cations have a large impact on

* Author for correspondence: patrick.garidel@t-online.de

1388–6150/$20.00

Akadémiai Kiadó, Budapest, Hungary
Springer, Dordrecht, The Netherlands

the phase behaviour of the lipid mixture [16, 17] and thus influence the overall property of the membrane.

The presented study directs its attention to the intrinsic lipid molecule interactions in model membranes, and how the phase behaviour and the mixing properties are determined. The mixing behaviour of lipids and the formation of inhomogeneities are reflected in the shape of the phase diagram. A phase diagram (temperature *vs*. composition diagram) describes the stability of various phases and their coexistence region. The temperatures separating a one-phase region (gel or liquid crystalline phase) from a two-phase region (coexistence of gel and liquid crystalline phase) are plotted as a function of composition at constant pressure. One of the most elegant methods to obtain data for the construction of phase diagrams is derived from calorimetric experiments by measuring the excess heat capacity as a function of temperature. The heat capacity curve represents the phase transition from one into another phase. For lipids, the main phase transition corresponds to the transition from a gel to the liquid crystalline phase. The onset and the end temperatures for the phase transition are determined as those temperatures corresponding to the intersection between the tangent of the leading edge ('tangent-method') and the baseline of the DSC curves or by the deviation of the heat capacity curve from the baseline. (Fig. 1) These temperatures are then corrected by the finite width of the transition of the pure components weighed with their mole fractions [18].

One major problem is, that all these empirical methods have a certain arbitrariness, and in some cases one has to switch from one method to another without scientifically sound justifications. For the phase transition of pure lipids like DMPC (1,2-dimyristoyl-*sn*-glycero-3-phosphocholine), the use of the 'tangent-method' seems to be justified due to extremely steep flanks (Fig. 1a). However, for other heat capacity curves the application of the 'tangent-method' is not clear (Fig. 1b). Therefore, one of the main difficulties to be solved is the definition of the onset ($T(-)$) and offset ($T(+)$) temperatures of the melting for every single transition curve in a standardized manner.

The aims of the presented work are the following:

- The presentation of a procedure for the determination of these temperatures ($T(-)$ and ($T(+)$) by the simulation of the heat capacity curves (c_p curves). The used calculation is based on regular solution theory assuming non-ideal mixing of the components and incorporating a parameter describing the broadening of the transition due to limited cooperativity.
- The phase diagrams are then constructed in a first approximation using the onset and offset temperatures obtained from the calculation of the heat capacity curves and further refined by a simulation procedure with a model using non-ideal, non-symmetric mixing behaviour in both phases.
- Various examples are shown for the mixing behaviour of pseudo binary phospholipid systems in excess water, as influenced by parameters like the ionic strength, pH of the buffer, and membrane composition.

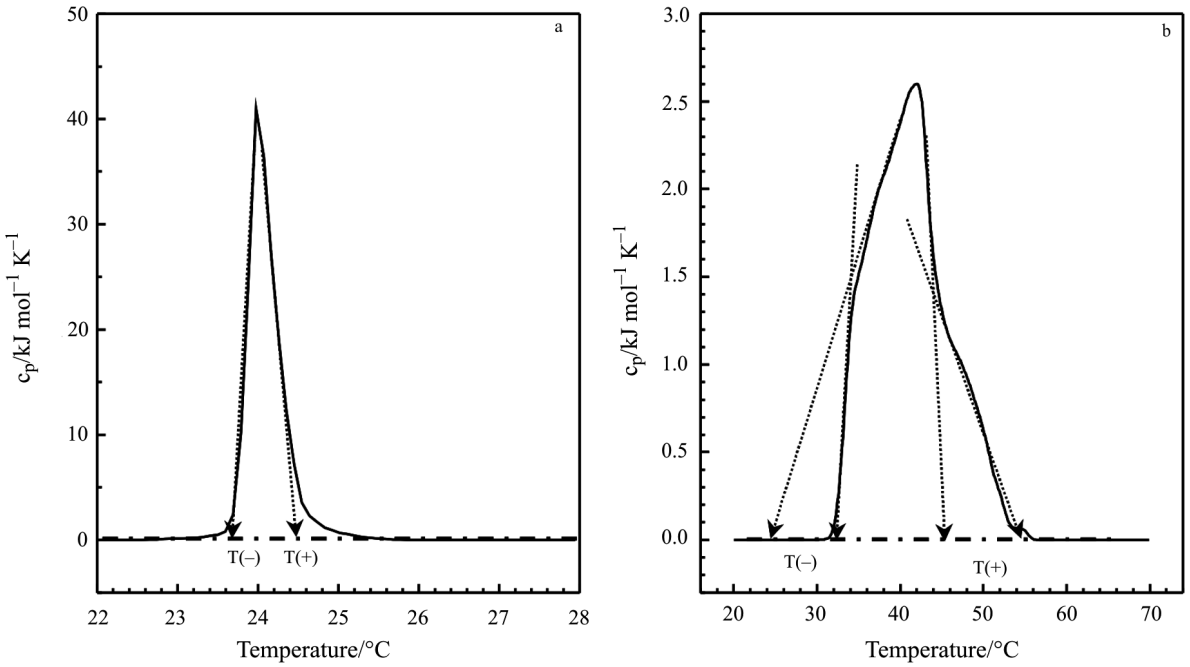

Fig. 1 The application of the 'tangent-method' for the determination of the onset and offset temperatures of the phase transition; a – sharp phase transition, b – broadened phase transition

Experimental

Materials and methods

The lipids used in this study were provided from Lipoid GmbH (Ludwigshafen, Germany), Nattermann Phospholipid GmbH (Cologne, Germany) and from Genzyme Pharmaceuticals Sygena Facility (Liestal, Switzerland): DMPA: 1,2-dimyristoyl-*sn*-glycero-3-phosphatidic acid, DPPA: 1,2-dipalmitoyl-*sn*-glycero-3-phosphatidic acid, DMPC: 1,2-dimyristoyl-*sn*-glycero3-phosphocholine, DPPC: 1,2-dipalmitoyl-*sn*-glycero3-phosphocholine, DMPE: 1,2-dimyristoyl-*sn*-glycero3-phosphoethanolamine, DPPE: 1,2-dipalmitoyl-*sn*-glycero-3-phosphoethanolamine, DMPG: 1,2-dimyristoyl-*sn*-glycero-3-phosphoglycerol (Na-salt), DPPG: 1,2-dipalmitoyl-*sn*-glycero-3-phosphoglycerol (Na-salt), The lipid mixtures were prepared according to a general protocol [19] and the DSC experiments were performed as described previously at a scanning rate of 1°C min^{-1} [19].

Calculation of the heat capacity curves c_p

The principle: The expression for the heat capacity c_p^{id} describing a hypothetical phase transition for binary lipid mixtures with infinitely high cooperativity [20, 21] with ideal mixing is calculated and combined in a second step with an expression taking into account the property of limited cooperativity. The latter effect induces a broadening of the heat capacity curve and is described by a 'cooperativity function' (dΘ/dT), which is folded with the c_p^{id} curve yielding the simulated heat capacity curve c_p^{sim} (Fig. 2).

Ideal heat capacity curve c_p^{id}: The molar enthalpy H of a binary lipid system in the phase transition region from one phase to another (e.g. gel (g) to the liquid crystalline (l) phase) is given by:

$$H=\varphi H_g+(1-\varphi)H_l \quad (1)$$

with H_g and H_l representing the enthalpies of the gel and liquid crystalline phase. φ describes the degree of transition going from 1 to 0 in the liquid crystalline phase and can be calculated from the lever rule [21]. This phase model assumes that the enthalpic effects are mainly initiated from changes of the hydrophobic interactions between acyl chains and that with increasing temperature the number of gauche conformers increases [22–24].

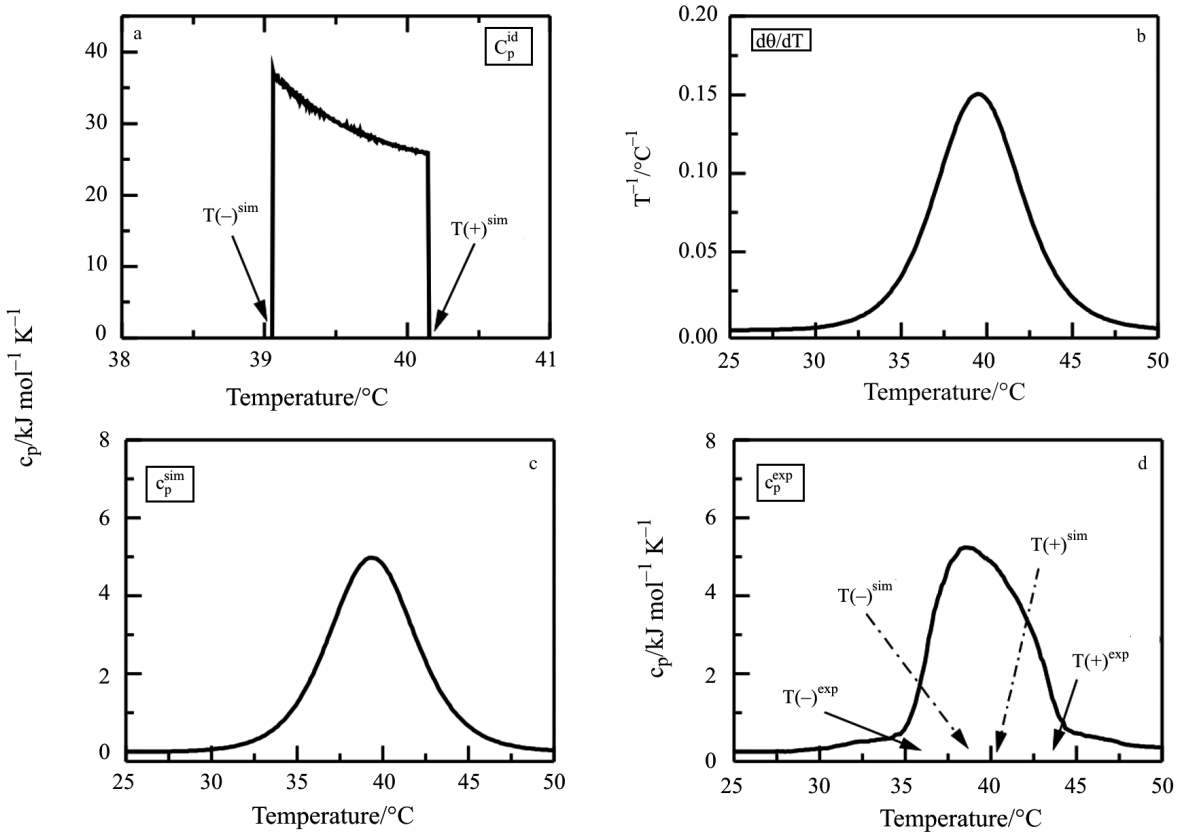

Fig. 2 Schematic representation for the simulation of a heat capacity curve. a – theoretical (ideal) heat capacity curve c_p^{id}, b – broadening function (dΘ/dT), c – simulated heat capacity curve c_p^{sim} after convolution d – experimental heat capacity curve. $T(-)^{exp}$ and $T(+)^{exp}$: onset and offset temperatures obtained by an empirical method and $T(-)^{sim}$ and $T(+)^{sim}$: onset and offset temperatures obtained by the simulation procedure (see text)

For each phase, assuming non-ideal mixing of the lipids (binary system with the components A and B), the enthalpies H_g and H_l as a function of composition are:

$$H_g=x_A H_{g,A}+x_B H_{g,B}+\Delta H_g^E ; H_l=x_A H_{l,A}+x_B H_{l,B}+\Delta H_l^E \quad (2)$$

with x_g being the mole fractions in the gel (g) and liquid crystalline (l) phase. ΔH^E is the excess enthalpy describing the deviation of the system from ideal mixing behaviour in each phase. These equations give an expression for the total enthalpy H of the system as a function of temperature [21]. ΔH^E is calculated from the Gibbs–Helmholtz equation for the free excess Gibbs energy of mixing ΔG^E.

In the frame of regular solution theory [25], the excess entropy is set to zero, and thus the excess free Gibbs energy of mixing equals the excess enthalpy of mixing. This approach is justified by the fact, that the shape of the lipid molecules is quite similar and that the non-ideality of the system is caused by a nonzero ΔH^E [8, 21].

In regular solution theory, ΔG^E is developed as a function of the mole fraction x:

$$\Delta G^E=\Delta H^E=x(1-x)\{\rho_1+\rho_2(2x-1)+\rho_3(2x-1)^2+...\} \quad (3)$$

using parameters ρ_j which describe the deviations from ideal mixing behaviour. Positive non-ideality parameters indicate a tendency towards cluster formation of like lipids (A–A and B–B), whereas negative non-ideality parameters indicate the formation of complexes of unlike molecules (A–B pairs) [26].

For the simulation of the heat capacity curves a symmetrical formulation for the excess enthalpy for both phases was used:

$$\Delta G^E=\Delta H^E=x(1-x)\rho \quad (4)$$

However, other approaches for the description of the heat capacity curves have been presented (for more detail we refer to Johann *et al.* [21]). Based on these equations, the solidus and liquidus curves, which are the border lines of the coexistence range can be calculated [21, 26, 27]. These two equations describe the temperature T for which the two phases are in equilibrium. The heat capacity curve $c_p^{id}=(dH/dT)_p$ can now be calculated once the segments of the liquidus and solidus curves of the phase diagram are known. The exact expressions can be found elsewhere [6, 21, 28]. As can be seen from Fig. 2A, c_p^{id} is only defined in the coexistence region, and is zero outside. c_p^{id} is a function with a very high heat capacity maximum and with an extremely reduced half-width (Fig. 2).

Cooperativity function ($d\Theta/dT$): For an infinitely cooperative phase transition the system undergoes a true phase change at a singular temperature, the resulting heat capacity curve shows an infinitely narrow half-width. In reality, the phase transition curves are broadened due to limited cooperativity (Fig. 1). Limited cooperativity, i.e. the broadening effect of the phase transition, is taken into account by assuming an equilibrium between the gel (g) and the liquid crystalline (l) phase. The equilibrium constant K for such a process is given by

$$K=[L]/[G]=(1-\Theta)/\Theta \quad (5)$$

Θ the degree of transition is running from 1 (all lipids in the g phase) to 0 (all lipids in the l phase). The amount of lipid in one state is represented by brackets. An expression for ($d\Theta/dT$) is obtained by using the van't Hoff equation. Thus, the broadening function (Fig. 2B) describing the width of the transition as a function of the van't Hoff transition enthalpy ΔH_{vH}, can be calculated [21, 29, 30].

Simulated heat capacity curve c_p^{sim} : The corrected heat capacity curve c_p^{sim} is obtained by convoluting the c_p^{id} curve with the broadening function ($d\Theta/dT$) (Fig. 2)

$$c_p^{sim}=c_p^{id}\otimes(d\Theta/dT) \quad (6)$$

The derived equations are implemented in a fit program for the simulation of experimental heat capacity curves [21, 28]. As input parameters, the main phase transition temperatures, the calorimetrically determined phase transition enthalpies ΔH_c of the pure components, and the composition of the mixtures are used.

As a result of the experimental DSC curve simulation procedure,

- the non-ideality parameters ρ_g and ρ_l (one for each phase),
- the temperature values describing the onset ($T(-)^{sim}$) and offset ($T(+)^{sim}$) of the phase transition,
- and the van't Hoff enthalpy ΔH_{vH} as a function of composition

are obtained. $T(-)^{sim}$ and $T(+)^{sim}$ are the temperatures defining the liquidus and solidus curves of the phase diagram. Additionally, a value for the cooperative unit size can be calculated, which reflects the number of molecules in a domain that change abruptly their physical state (gel to liquid crystalline state) [6, 7].

Phase diagram simulation

Various approaches (e.g. quasi-chemical approaches) are used for the simulation of phase diagrams [20, 22, 31, 32]. The published simulation procedure based on regular solution theory utilises in most cases only one adjustable parameter, and assumes symmetric mixtures [26, 27, 33, 34]. However, more realistic is that the non-ideality parameters are a function of composition. This leads to a model with non-symmetric, non-ideal mixing behaviour.

To account for this, in an additional optimisation of the model, the phase diagrams were simulated using an approach for non-ideal, non-symmetric mixing with two non-ideality parameters for each phase [21]:

$$\Delta G^{E}=\Delta H^{E}=x(1-x)[\rho_1+\rho_2(2x-1)] \quad (7)$$

Applications and discussion

The presented approach has been used for a number of systems composed of a binary mixture of phospholipids in excess buffer, so called pseudo-binary systems [19–21]. Figure 2 summarizes graphically the concept used for the simulation of the heat capacity curves. From the simulation of the heat capacity curve, $T(-)^{sim}$ and $T(+)^{sim}$ are obtained, and as expected, these temperatures are much closer together than those obtained by the usual empirical procedure ($T(-)^{exp}$ and $T(+)^{exp}$) (Fig. 2D). In Fig. 3 examples are shown for the simulation of heat capacity curves of pseudo-binary phospholipid mixtures composed of DMPE and DMPG at pH 7 in 0.1 M NaCl. The experimental heat capacity curves (solid lines in Fig. 3) were taken in the heating mode at a scan rate of 1°C min^{-1}, representing the phase transition from the gel to the liquid crystalline phase. At scan rates >5°C min^{-1}, the phase transitions become broader due to kinetic effects of the phase transition. Additionally instrumental sensitivity and responses have to be considered (for more details, see discussions in [19, 28]). For the shown examples in this paper (phospholipid-phospholipid systems), the heat capacity curve as obtained from the cooling scan is nearly identical compared to the heat capacity curve obtained from the heating scan. No hysteresis is observed. Due to the fact, that the cooling scan represents the phase transition from the liquid crystalline to the gel phase, the enthalpy contributions are similar, however opposite in sign; an endothermic phase transition in the heating mode is detected as an exothermic phase transition in the cooling mode and vice versa.

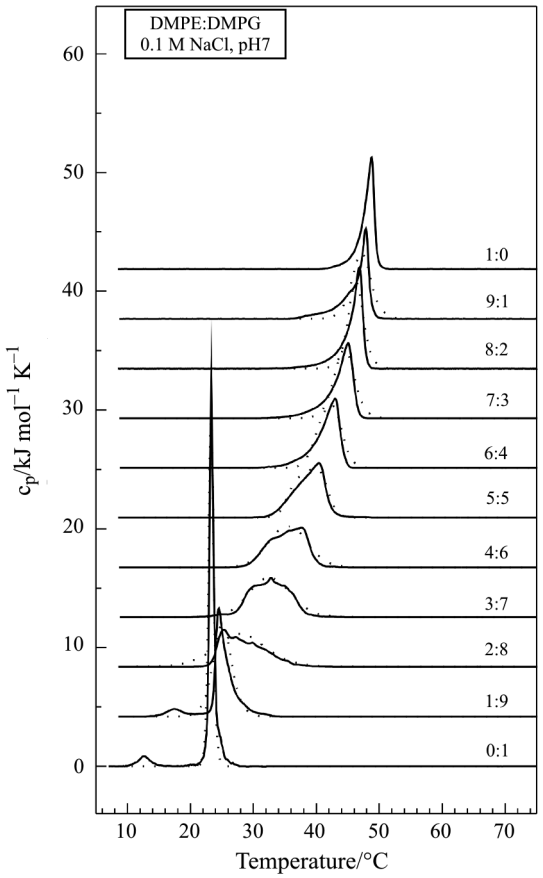

Fig. 3 DSC heating curves for DMPE:DMPG mixtures of various compositions at pH 7 in 0.1 M NaCl, solid lines: experimental c_p curves and dotted lines: c_p^{sim} curves (adapted from [35])

Pure phosphatidylglycerols show two phase transitions. The so-called pre-transition (T_p~13°C for DMPG at pH 7 in 0.1 M NaCl) stands for a transition between two gel phases ($L_{\beta'}\rightarrow P_{\beta'}$) (Fig. 3 bottom heat capacity curve). The main phase transition (T_m~23°C for DMPG at pH 7 in 0.1 M NaCl [36]) represents the transition from the $P_{\beta'}$ gel to the liquid crystalline L_α phase, which is characterised by a large increase of gauche conformers of the hydrocarbon chains and by an increased lateral diffusion of the single lipids within the membrane. The simulation of the heat capacity curves used here considers only the main phase transition (discussion in [6, 21]). The experimental curves are drawn as solid lines; the simulated heat capacity curves are represented by dotted lines (Fig. 3). As can be seen the obtained c_p^{sim} curves fit very well with the experimental curves. The calculated on- and offset temperatures as obtained from the simulation of the heat capacity curves of the DMPE:DMPG mixtures are shown in Fig. 4 as triangles: $T(-)^{sim}$ (open triangle) and $T(+)^{sim}$ (solid triangle). Additionally, the onset and offset temperatures are shown as obtained from the empirical method. These data are designated as: $T(-)^{exp}$ (open circle) and $T(+)^{exp}$ (solid circle). From Fig. 4, it is obvious, that both temperature sets deviate considerably from each other, especially for phospholipid mixtures $x_{DMPG}<0.4$ [35]. Based on $T(-)^{sim}$ and $T(+)^{sim}$ the coexistence curves are calculated using the non-ideal, non-symmetric model (Fig. 4).

The shape of a phase diagram depends mainly on the intermolecular interactions and thus mixing behaviour of the components in both phases. Ideal miscibility of two components in both phases, is denoted by solidus and liquidus curves enclosing a 'cigar like' coexistence region of both phases. Below the solidus curve only the gel phase is existent, and above the liquidus line only a

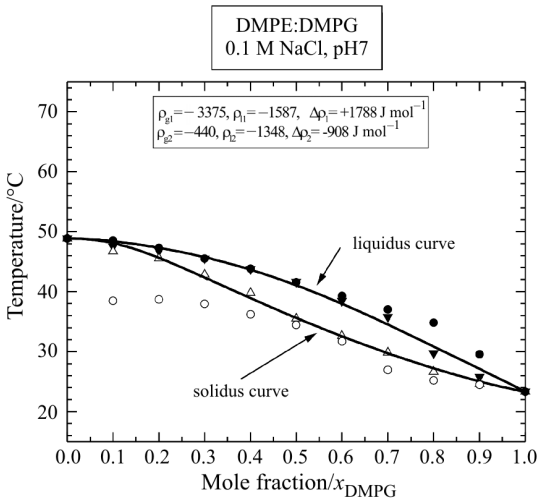

Fig. 4 Phase diagram for the system DMPE:DMPG at pH 7 in 0.1 M NaCl, constructed from the c_p^{sim} curves. The solid lines are coexistence lines calculated using the four-parameter non-ideal, non-symmetric mixing model described in the text. Circles: on- and offset temperatures obtained from the empirical method. Triangles: on- and offset temperatures obtained from the simulation of the experimental heat capacity curves (adapted from [35])

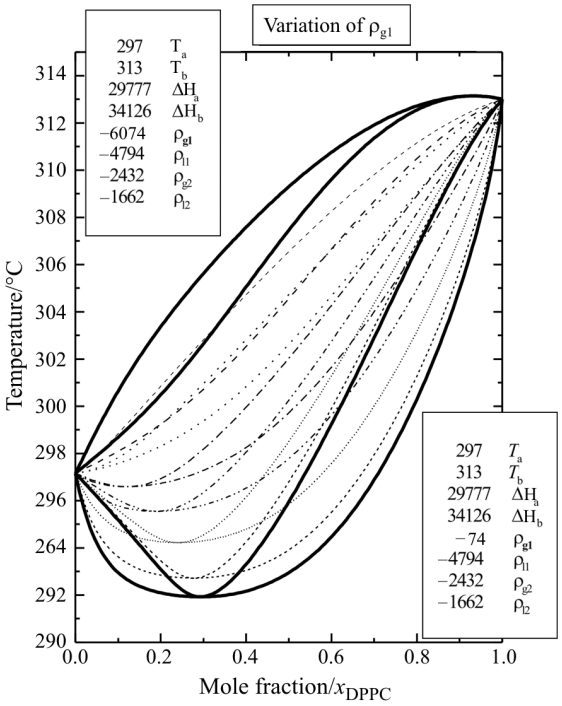

Fig. 5 Simulation of the phase diagram of the binary lipid system DMPC:DPPC (pH 7, water) using the four-parameter non-ideal, non-symmetric mixing model, however, without taking into account on- and offset temperatures (see text). All simulation parameters (ρ_{g2}, ρ_{l1}, ρ_{l2},) were fixed with the exception of ρ_{g1}, which was varied consecutively. The ρ-data are summarised in the boxes. The resulting solidus and liquidus curves are shown. T in K, ΔH in J mol^{-1}, ρ in J mol^{-1}. Simulation # 1: top, simulation # 8: bottom

liquid crystalline phase appears (Fig. 6). Such an ideal mixing behaviour is found for DMPG:DPPG mixtures (pH 7, 0.1 M NaCl) with the non-ideality parameters being zero [7]. Other examples of ideally miscible phospholipids are known, e.g. DMPC:DPPC, or DMPE:DPPE [36]. These are examples for systems having the same head groups with the hydrocarbon chains varying only by two methylene units. However, ideal mixing behaviour has also been described for systems with different head groups, but with identical chain length e.g. DMPC:DMPG or DPPC:DPPG [7, 37]. Non-ideal mixing with the formation of domains in the gel phase can be induced by increasing the acyl chain length of one component by more than four methylene units, e.g. DMPC:DSPC [26, 38–41].

The system DMPE:DMPG (pH 7, 0.1 M NaCl) (Fig. 4) shows deviations from ideality at low molar ratios of DMPG. The non-ideality parameters obtained from the simulation are:

$$\rho_{g1}= -3375, \rho_{l1}= -1587, \rho_{g2}= -440, \rho_{12}= -1348 \text{ J mol}^{-1}.$$

In both phases DMPE-DMPG lipid pair formation is favoured (negative ρ data) and is more pronounced for the gel phase ($\rho_{g1}<\rho_{l1}$). The differences in the non-ideality parameters between liquid crystalline and gel phase

$$\Delta\rho_1=\rho_{l1}-\rho_{g1} \text{ and } \Delta\rho_2=\rho_{l2}-\rho_{g2} \quad (8)$$

are: $\Delta\rho_1$=+1788 and $\Delta\rho_2$= –908 J mol^{-1}. The parameter $\Delta\rho_2$ describes the difference in asymmetry in the mixing behaviour between both phases and vanishes at x=0.5 (Eq. (7)).

At pH 7, the mixtures in the liquid crystalline phase show a smaller deviation from ideal mixing, compared to the non-ideality parameter of the gel phase ($\rho_1<0$, $\rho_{l1}>\rho_{g1}$), with both non-ideality parameters having negative values. Negative non-ideality parameters indicate the preference of pair formation of unlike molecules. The asymmetry for both phases is larger for the liquid crystalline phase compared to the gel phase, indicating a stronger composition dependence for the liquidus line.

For the calculation of the phase diagram, a set of on- and offset temperatures is required for the correct construction of the phase diagrams. In Fig. 5 an example is shown (DMPC:DPPC) for which no on- and offset data are used. As starting values for the simulation, the thermodynamic data of both pure components are used (main phase transition and main phase transition enthalpy), with fixed values for ρ_{l1}, ρ_{l2} and ρ_{g2}, whereas ρ_{g1} has been varied (increment variation for ρ_{g1}=500 J mol^{-1}) (selected data are shown in Fig. 5). The differences in the non-ideality parameters between liquid crystalline and gel phase are for the simulation # 1 (top lines in Fig. 5): $\Delta\rho_1$= +1280 and $\Delta\rho_2$ = +770 J mol^{-1} and for the simulation # 8 (bottom

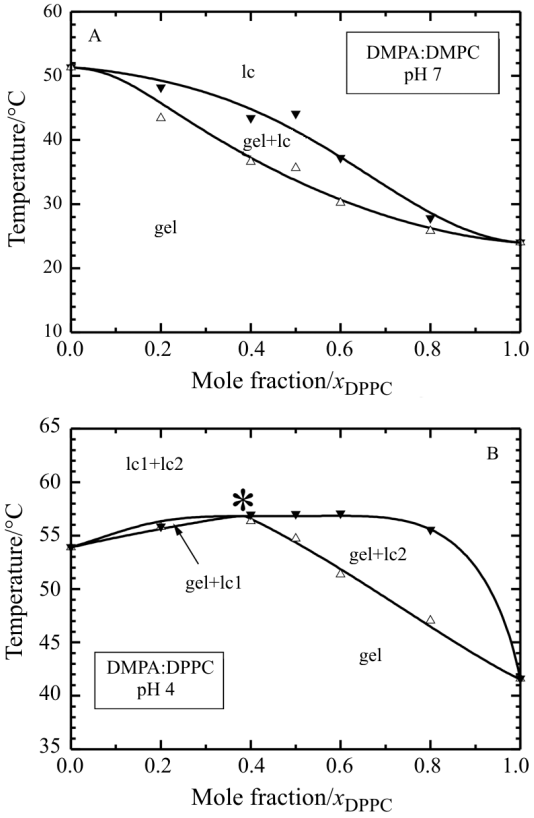

Fig. 6 Phase diagrams for A – DMPA:DMPC at pH 7 (water) and B – DMPA:DPPC at pH 4 (water) constructed from the c_p^{sim} curves. The solid lines are coexistence lines calculated using the four-parameter non-ideal, non-symmetric mixing model described in the text. Triangles: on- and offset temperatures obtained from the simulation of the experimental heat capacity curves. Gel: gel phase, lc: liquid crystalline phase, *: azeotropic point

lines in Fig. 5): $\Delta\rho_1 = -4720$ and $\Delta\rho_2 = +770$ J mol^{-1}, indication stronger deviations from non-ideality for the case # 8 compared to #1. Therefore, on- and offset data obtained from the simulation of the heat capacity curve are required for the correct construction of phase diagrams.

The examples shown in Fig. 6 are calculated using $T(-)^{sim}$ and $T(+)^{sim}$ (triangle symbols in Fig. 6) [6]. With these two examples, the influence of pH or chain length composition of the lipids is discussed.

In phosphatidic acids (e.g. DMPA), the charge of the head group can be modulated by changes in pH, ionic strength, or the presence of divalent cations, influencing the molecular interaction with other lipids, and thus changing the lipid mixing behaviour [42, 43]. This is reflected in changes in the shape of the phase diagrams. At pH 7 (water) DMPA is singly charged, whereas at pH 4 the head group is partly protonated [44, 45]. The charge of zwitterionic phosphatidylcholines is not affected by changing the pH from 7 to 4, because the pK of the phosphodiester group is much lower [3].

At pH 7, DMPA:DMPC as well as DMPA:DPPC mixtures (data not shown) show a deviation from ideal mixing behaviour [6]. However, protonation of DMPA (at pH ~ 4, approximately -0.6 elementary charges) [44, 45] changes the mixing behaviour of this system completely, versus an increase in the non-ideal mixing behaviour of the two components. This effect is further enhanced by a variation of the hydrocarbon chain length of one component (Fig. 6b: DMPA:DPPC system). The phase diagram of the system DMPA:DPPC at pH 4 (Fig. 6B) indicates that either an azeotropic point at x_{DPPC}=0.38, where the liquidus and the solidus curve touch, or even an immiscibility region in the liquid crystalline phase between $x_{DPPC} \approx 0.3$ and $x_{DPPC} \approx 0.7$ is formed. This is indicated by the horizontal part of the liquidus line in this composition range. The assumption of a miscibility gap in the liquid crystalline phase means that the formation of fluid lipid domains with different compositions (lc1 and lc2) has to be considered (large and positive ρ_{11} are obtained, for more details see [6]). Protonation of DMPA (pH 4) induces a reduction of the electrostatic repulsion between the DMPA molecules. Furthermore, intermolecular interactions in the polar head groups are increased due to the enhanced ability for the formation of a hydrogen bonding network. As a consequence of the changed intermolecular interactions, a tendency for the formation of inhomogeneities *vs.* demixing and the formation of microdomains of different composition is favoured.

Wu and McConnell (1975) [46] first postulated liquid–liquid phase separation in a DEPC/DPPE system, but these results were later contradicted by Silvius [47].

The concept of liquid-liquid immiscibility has gained of significance in the last years, and efforts were undertaken to discover other systems with this behaviour. Examples showing liquid-liquid immiscibility were found e.g. in systems composed of two phosphatidylcholines where one of the components has highly asymmetric chains [48] and in mixtures of phosphatidylcholine with phosphatidylserine [49]. The phosphatidylcholine-phosphatidylserine example published by Hinderliter *et al*. [49] is similar to the DMPA:DPPC (pH 4) system, because the electrostatic repulsion between phosphatidylserine molecules in phosphatidylcholine-phosphatidylserine mixtures [49] seems to be overcompensated by other attractive interactions, giving rise to clustering of like molecules. A similar behaviour has also been found for the system DPPC:DMPG by changing the pH from 7 to 2 [7]. These examples are of particular interest, because fluid-fluid immiscibility can be triggered by only changing the pH. Monte Carlo techniques can be used for the illustration of the formation of liquid-liquid domains [6, 50, 51].

The mixing behaviour of lipids can be changed by a number of external factors as the presence of divalent cations or buffer composition and ionic strength (for more details consult [52–56]). The relevance of inhomogeneities for biological functions has received increasing interest [57–60] and shows that the proposed fluid-mosaic model by Singer and Nicholson has to be refined.

Conclusions

A procedure is described for the objective determination of the onset and offset temperatures of melting curves obtained from calorimetric measurements by fitting the experimental heat capacity curves using one non-ideality parameter for each phase and an additional parameter which takes into account the broadening of the heat capacity curves due to limited cooperativity of the phase transition. From the simulation on- and offset temperatures are obtained, which are used for the construction of the phase diagram. In a next step the phase diagram is refined using a thermodynamic model considering non-ideal and non-symmetric mixing in each phase (regular solution theory). The presented examples illustrate the usefulness of such an approach for the analysis of phospholipid pseudobinary systems.

Acknowledgements

This work was supported by the Deutsche Forschungsgemeinschaft (Bl 182/7-3) and the Fonds der Chemischen Industrie.

References

1 E. Gorter and F. Grendel, J. Exp. Med., 41 (1925) 439.
2 A. S. Janoff (Ed.), Liposomes. Rational design, Marcel Dekker Inc., New York and Basel, 1999.
3 G. Cevc (Ed.), Phospholipids Handbook, Marcel Dekker Inc., New York and Basel 1993.
4 H. J. Galla and E. Sackmann, J. Am. Chem. Soc., 97 (1975) 4114.
5 A. G. Lee, N. J. M. Birdsall, J. C. Metcalfe, P. A. Toon and G. B. Warren, Biochemistry, 13 (1974) 3699.
6 P. Garidel, C. Johann and A. Blume, Biophys. J., 72 (1997) 2196.
7 P. Garidel, C. Johann, L. Mennicke and A. Blume, Eur. Biophys. J., 26 (1997) 447.
8 M. Edidin, Ann. Rev. Biophysics Biomol. Structure, 32 (2003) 257.
9 S. Munro, Cell, 115 (2003) 377.
10 K. Gaus, E. Gratton, E. P. W. Kable, A. S. Jones, I. Gelissen, L. Kritharides and W. Jessup, Proc. Natl. Acad. Sci., 100 (2003) 15554.
11 H. Heerklotz, Biophys. J., 83 (2002) 2693.
12 H. Heerklotz, H. Szadkowska, T. Anderson and J. Seelig, J. Mol. Biol., 329 (2003) 793.
13 C. Dietrich, L. A. Bagatolli, Z. N. Volovyk, N. L. Thompson, M. Levi, K. Jacobson and E. Gratton, Biophys. J., 80 (2001) 1417.
14 R. C. Aloia and J. M. Boggs (Eds), Membrane fluidity in biology, Vol. 4, Cellular aspects, Academic Press Inc., London 1985.
15 R. C. Aloia, C. C. Curtain and L. M. Gordon, Advances in membrane fluidity, Vol. 1–3, Alan R. Liss, Inc., New York 1988.
16 P. Garidel and A. Blume, Langmuir, 16 (2000) 1662.
17 P. Garidel, C. Johann and A. Blume, Liposome Res., 8 (1998) 58.
18 S. Mabrey and J. M. Sturtevant, Proc. Natl. Acad. Sci. USA, 73 (1976) 3862.
19 A. Blume and P. Garidel, (1999) Lipid model membranes and biomembranes. In: P. K. Gallagher (series Ed.), The Handbook of Thermal Analysis and Calorimetry, R. B. Kemp (Ed.), From Macromolecules to man, 1st Ed., Vol. 4, Elsevier Amsterdam, p. 109.
20 A. G. Lee, Biochim. Biophys. Acta, 472 (1977) 237.
21 C. Johann, P. Garidel, L. Mennicke and A. Blume, Biophys. J., 71 (1996) 3215.
22 A. G. Lee, Biochim. Biophys. Acta, 472 (1977) 285.
23 S. W. Rick, J. Phys. Chem. B, 107 (2003) 9853.
24 A. G. Lee, Biochim. Biophys. Acta, 507 (1978) 433.
25 H. J. Hildebrandt, J. Am. Chem. Soc., 51 (1929) 66.
26 B. Tenchov, Prog. Surf. Sci., 20 (1985) 273.
27 E. E. Brumbaugh and C. Huang, Methods Enzym., 210 (1992) 521.
28 P. Garidel, C. Johann and A. Blume, J. Liposome Res., 10 (2000) 131.
29 A. Blume, Applications of calorimetry to lipid model membranes. In: Physical properties of biological membranes and their functional implications. C. Hidalgo, editor. Plenum Publishing Corporation, New York 1988.
30 A. Blume, Thermochim. Acta, 193 (1991) 299.
31 P. H. van Dreele, Biochemistry, 17 (1978) 3939.
32 S. C. Chen, J. M. Sturtevant and B. J. Gaffney, Proc. Natl. Acad. Sci. USA, 77 (1980) 5060.
33 J. H. Ipsen and O. G. Mouritsen, Biochim. Biophys. Acta, 944 (1988) 121.
34 E. E. Brumbaugh, M. L. Johnson and C. Huang, Chem. Phys. Lipids, 52 (1990) 69.
35 P. Garidel and A. Blume, Eur. Biophys. J., 28 (2000) 629.
36 P. Garidel and A. Blume, Biochim. Biophys. Acta, 1371 (1998) 83.
37 Y. Nibu, T. Inoue and I. Motoda, Biophys. Chem., 56 (1995) 273.
38 W. Knoll, K. Ibel and E. Sackmann, Biochemistry, 20 (1981) 6379.
39 O. G. Mouritsen, Chem. Phys. Lipids, 57 (1991) 179.
40 C. Gliss, H. Clausen-Schumann, R. Günther, S. Odenbach, O. Randl and T. M. Bayerl, Biophys. J., 74 (1998) 2443.
41 I. P. Sugár, T. E. Thompson and R. L. Biltonen, Biophys. J., 76 (1999) 2029.
42 P. Garidel and A. Blume, Langmuir, 15 (1999) 5526.
43 A. Blume and J. Tuchtenhagen, Biochemistry, 31 (1992) 4636.

44 A. Blume and H. Eibl, Biochim. Biophys. Acta, 558 (1979) 13.
45 H. Eibl and A. Blume, Biochim. Biophys. Acta, 553 (1979) 476.
46 S. H. Wu and H. M. McConnell, Biochemistry, 14 (1975) 847.
47 J. R. Silvius, Biochim. Biophys. Acta, 857 (1986) 217.
48 J. T. Mason, Biochemistry, 27 (1988) 4421.
49 A. K. Hinderliter, J. Huang and G. W. Feigenson, Biophys. J., 67 (1994) 1906.
50 K. Kawasaki, Kinetics of Ising models. In: Phase Transitions and Critical Phenomena. C. Domb and M. S. Green, Eds Academic Press, London 1972, p. 443.
51 H. Jan, T. Lookman and D. A. Pink, Biochemistry, 23 (1984) 3227.
52 K. Jørgensen and O. Mouritsen, Biophys. J., 69 (1995) 942.
53 K. Lohner, A. Latal, G. Degovics and P. Garidel, Chem. Phys. Lipids, 111 (2001) 177.
54 J. F. Tocanne, Comm. Mol. Cell. Biophys., 8 (1972) 53.
55 M. Glaser, Curr. Opin. Struct. Biol., 3 (1993) 475.
56 T. Dewa, Y. Miyake, F. J. Kézdy and S. L. Regen, Langmuir, 16 (2000) 3735.
57 R. F. M. De Almeida, A. Fedorov and M. Prieto, Biophys. J., 85 (2003) 2406.
58 L. H. Chamberlain, FEBS Letters, 559 (2004) 1.
59 W. H. Binder, V. Barragan and F. M. Menger, Angew. Chem., 115 (2003) 5980.
60 B. Pozo Navas, K. Lohner, G. Deutsch, E. Sevcsik, K. A. Riske, R. Dimova, P. Garidel and G. Pabst, Biochim. Biophys. Acta, 1716 (2005) 40.

DOI: 10.1007/s10973-005-7239-x